

Research Article

Comparative Solid Phase Photocatalytic Degradation of Polythene Films with Doped and Undoped TiO₂ Nanoparticles

Wasim Asghar,¹ Ishtiaq A. Qazi,¹ Hassan Ilyas,¹ Aftab Ahmad Khan,² M. Ali Awan,¹ and M. Rizwan Aslam¹

¹*Institute of Environmental Science and Engineering, School of Civil and Environmental Engineering, National University of Sciences and Technology (NUST), Sector H-12, Islamabad 44000, Pakistan*

²*Advanced Engineering Research Organization (AERO), Hassan Abdal 43730, Pakistan*

Correspondence should be addressed to Wasim Asghar, wasim@iese.edu.pk

Received 19 February 2010; Accepted 14 April 2010

Academic Editor: Bo Zou

Copyright © 2011 Wasim Asghar et al. This is an open access article distributed under the Creative Commons Attribution License, which permits unrestricted use, distribution, and reproduction in any medium, provided the original work is properly cited.

Comparative photocatalytic degradation of polythene films was investigated with undoped and metal (Fe, Ag, and Fe/Ag mix) doped TiO₂ nanoparticles under three different conditions such as UV radiation, artificial light, and darkness. Prepared photocatalysts were characterized by XRD, SEM, and EDS techniques. Photocatalytic degradation of the polythene films was determined by monitoring their weight reduction, SEM analysis, and FTIR spectroscopy. Weight of PE films steadily decreased and led to maximum of 14.34% reduction under UV irradiation with Fe/Ag mix doped TiO₂ nanoparticles and maximum of 14.28% reduction under artificial light with Ag doped TiO₂ nanoparticles in 300 hrs. No weight reduction was observed under darkness. Results reveal that polythene-TiO₂ compositing with metal doping has the potential to degrade the polythene waste under irradiation without any pollution.

1. Introduction

Titanium dioxide (TiO₂) is one of the most well-known efficient photocatalysts. The capability of TiO₂-based photocatalyst to degrade gaseous and aqueous contamination makes it a good candidate for use in air clean up and water purification. However, most applications so far are limited to UV light irradiation because the light absorption edge of pure TiO₂ is lower than 380 nm. Therefore, the development of modified titania with high activity under visible light ($\lambda > 380$ nm) should take full advantage of the main part of the solar spectrum (mostly 400–600 nm) [1].

The most promising approach of activation of TiO₂, in the visible light region, is modification of its chemical structure to shift the absorption spectrum to the visible light region [2–4]. This type of modification involves introduction of doping with metal and nonmetal species. To prepare an effective visible light, active photocatalyst doping should produce states in the band gap of TiO₂ that absorbs visible light [5].

The process of recycling polymers is expensive and time consuming; only a small percentage of the plastic waste is currently being recycled [6]. Biodegradable plastics have shown considerable promise in this context [7, 8]. However, the biodegradable plastics till now cannot completely solve the problem due to their chemical stability and nonaffordable cost [9]. More recently, photo degradation of plastics has also started receiving attention. The composition of plastic and TiO₂ nanoparticles (NPs) has been proven to be a new and useful way to decompose solid polymer in open air. Investigations on the photo degradation of polyvinyl chloride (PVC), polystyrene (PS), and polythene (PE) have been carried out [10–12]. More specifically, a few recent reports describe the use of TiO₂ and goethite and so forth as the photocatalyst for oxidative degradation of PE with very encouraging results [13, 14].

The present study was focused on solid phase photocatalytic degradation of polyethylene plastic with TiO₂ as photocatalyst and Fe, Ag metals as dopants. PE-TiO₂ composite films were prepared and their photocatalytic

degradation under ultraviolet irradiation, artificial light and darkness was studied.

2. Materials and Methods

2.1. Chemical Reagents. GPR TiO₂ (BDH Chemicals Ltd., England) and chemical reagents like iron (III) nitrate nonahydrate, silver nitrate, and cyclohexane (Merck, Germany) were used in this study. All chemicals were of analytical grade and used without further purification. PE originating from QAPCO Petrochemical Corp., Qatar was purchased from the local market.

2.2. Preparation of Doped TiO₂ Nanoparticles. Fe doped, Ag doped, and Fe/Ag mix doped TiO₂ NPs were prepared by the liquid impregnation (LI) method by the following steps. 3 g of GPR TiO₂ was added to 100 mL distilled water and then the required amount of iron (III) nitrate nonahydrate, for doping, was added to TiO₂ suspension, where the Fe concentration was of 1% (mole ratio) versus TiO₂. The slurry was stirred well and allowed to rest for 24 hours and then dried in an air oven at 100°C for 12 hours [15]. The dried solids were ground in an agate mortar and calcinated at 500°C for 3 hours in a furnace. Same steps were repeated with silver nitrate as precursor for Ag doped TiO₂ NPs where the Ag concentration was of 1% (mole ratio) versus TiO₂. For Fe/Ag mix doped TiO₂, iron (III) nitrate nonahydrate and silver nitrate were used as the precursors for Fe and Ag, respectively. The mole ratio, with respect to TiO₂, for both Fe and Ag was 0.5% each. GPR TiO₂ was calcinated at 500°C for 3 hours when used as undoped TiO₂ NPs source.

2.3. Preparation of PE-TiO₂ Composite Films. Polymer stock solution was prepared by dissolving 1 g of PE in 100 mL cyclohexane at 70°C under vigorous stirring for 60 minutes. Following this, TiO₂ NPs were suspended uniformly in the above solution to give 1.0% (weight) contents with respect to the total mass of PE. An aliquot of 20 mL of PE-TiO₂ prepared solution was spread as a disc ($r = 4$ cm) on a glass plate and first dried for 20 minutes at 70°C, then dried for 48 hours at room temperature [16]. Weight of the resulting PE-TiO₂ composite films was 0.2 gm approximately. Same procedure was followed to prepare the composite films of PE with Fe, Ag, and Fe/Ag mix doped TiO₂ NPs.

3. Characterization

3.1. Characterization of TiO₂ Nanoparticles

3.1.1. X-Ray Diffraction Analysis. Crystal size of the prepared photocatalyst was studied by powder XRD technique. X-ray diffraction patterns were obtained on JEOL JDX-II X-ray diffractometer using Cu-K_α radiation at an angle of 2θ from 10° to 80°. The crystallite size was determined from the X-ray diffraction patterns, based on the Scherer equation [14]

$$L = \frac{k\lambda}{\beta \cos \theta} \quad (1)$$

TABLE 1: Crystal sizes of doped and undoped TiO₂ nanoparticles.

Sr. no.	Sample name	Crystal size (nm)	
		Maximum	Minimum
1	Undoped TiO ₂	42.52	26.72
2	Fe doped TiO ₂	42.52	26.72
3	Ag doped TiO ₂	42.52	11.27
4	Fe/Ag mix doped TiO ₂	42.52	20.09

where k is a shape factor = 0.9, λ is the radiation wavelength = 1.54051° A, θ is the Bragg angle, β = full width of a diffraction line at one half of maximum intensity in radian.

3.1.2. SEM Study. SEM study of doped and undoped TiO₂ NPs was conducted with JEOL JSM-6460 scanning electron microscope to see the distribution of metal on the surface of TiO₂ in doped species.

3.1.3. EDS Analysis. Energy dispersive spectroscopic (EDS) analysis was conducted with Oxford INCA X-sight 200 to perform the quantitative analysis of the TiO₂ both in doped and undoped conditions.

3.2. Characterization of Polythene Films

3.2.1. Weight Reduction Analysis. Photo degradation study of the PE films was conducted based on weight reduction. Weighing balance, with 0.0001 gm sensitivity (Denver Instrument Company XE Series, model 100A) was used for weight measurements.

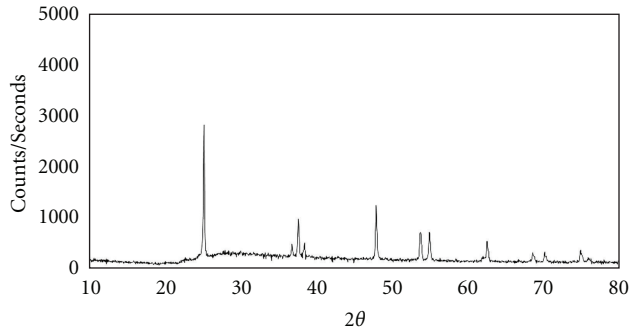
3.2.2. Surface Morphology and Thickness Analysis. Surface morphology & thickness analysis of PE films was conducted with JEOL JSM-6460 scanning electron microscope before and after the 300 hours of UV exposure.

3.2.3. FTIR Analysis. To get the qualitative analysis of the PE films, FTIR analysis was conducted with Perkin Elmer Spectrum BX-II FTIR spectrometer before and after irradiation.

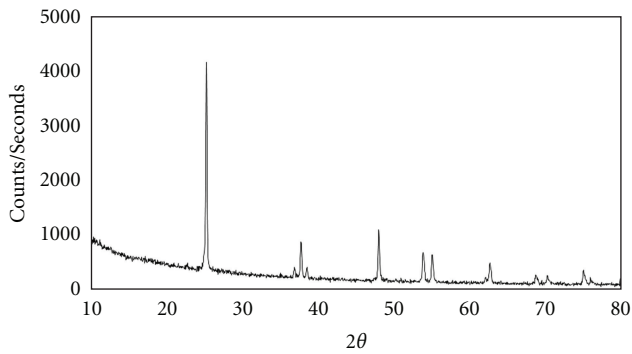
4. Results and Discussions

4.1. Characterization of TiO₂ Nanoparticles

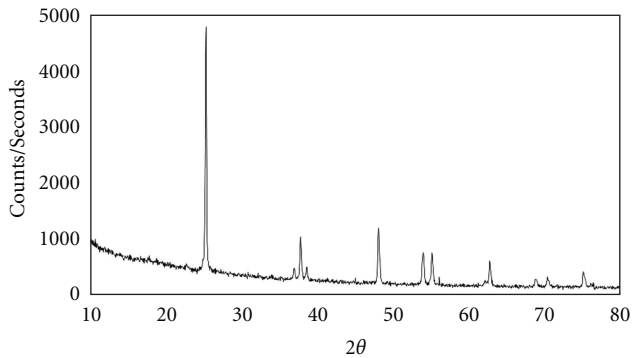
4.1.1. X-Ray Diffraction Analysis. Table 1 shows the results of X-ray diffraction analysis, which demonstrate a variation in nanoparticles size as compared to a previous study [15]. This study reported that the average size of prepared Ag doped TiO₂ NPs was 14 nm while Ag doped TiO₂ NPs prepared in current study were in the 11.27 to 42.52 nm range. This difference may be due to the TiO₂ source, as GPR TiO₂ was used as TiO₂ source in the current study while P-25 Degussa was used in the previous one. Figure 1 shows the respective XRD patterns of doped and undoped TiO₂ NPs.



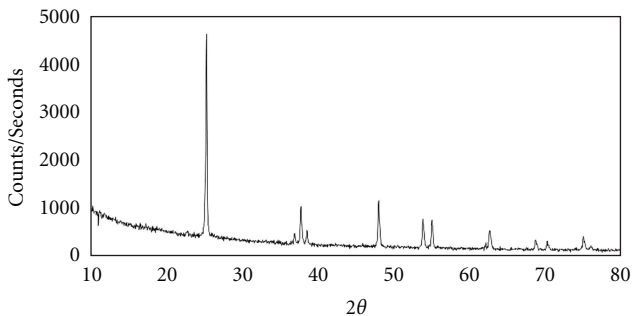
(a)



(b)



(c)



(d)

FIGURE 1: XRD patterns: (a) undoped TiO₂, (b) Fe doped TiO₂, (c) Ag doped TiO₂, and (d) Fe/Ag mix doped TiO₂.

TABLE 2: EDS analysis of doped and undoped TiO₂ nanoparticles.

Sr. no.	Sample name	Elements in percent ratio		
		Ti	Fe	Ag
1	Undoped TiO ₂	100.00	—	—
2	Fe doped TiO ₂	99.08	0.92	—
3	Ag doped TiO ₂	99.09	—	0.91
4	Fe/Ag mix doped TiO ₂	98.99	0.48	0.53

TABLE 3: Photo catalyzed weight reduction (maximum) of pure PE films and PE-TiO₂ composite films.

Sr. no.	Sample name	Maximum weight reduction (%)		
		UV	Artificial light	Dark
1	Pure PE	3.32	0.65	No reduction
2	PE + TiO ₂	10.6	6.51	= do =
3	PE + Fe doped TiO ₂	13.49	11.9	= do =
4	PE + Ag doped TiO ₂	13.75	14.28	= do =
5	PE + Fe/Ag mix doped TiO ₂	14.34	13.18	= do =

4.1.2. SEM Analysis. Figure 2 shows the images of doped and undoped TiO₂ NPs obtained with scanning electron microscope. These images show that the distribution of the dopant metals on the surface of TiO₂ is not uniform and doped species contain irregular shaped particles which are aggregations of tiny crystals. SEM analysis verifies the results of previous reported work [15].

4.1.3. EDS Analysis. Figure 3 shows the EDS spectra of doped and undoped TiO₂ NPs. EDS analysis shows that the percent composition is not consistent in the doped TiO₂ NPs. It varies from point to point showing that composition of the prepared NPs is not homogeneous. It confirms the SEM results. Average composition of doped and undoped NPs is given as in Table 2.

4.2. Characterization of Polythene Films

4.2.1. Weight Reduction Analysis. Pure PE and PE-TiO₂ composite films were exposed with UV and artificial light constantly for 300 hours under ambient conditions. Parallel studies were conducted with no irradiation under darkness. TiO₂ photocatalyst absorbs only UV light ($\lambda < 380$ nm), thus only UV light plays a role in solar degradation of PE-TiO₂ composite plastic. In order to reveal the photocatalytic degradation behavior the photo degradation reaction was conducted under ambient air in a lamp-housing box (50 cm × 40 cm × 30 cm) as shown in Figure 4. Pure PE and PE-TiO₂ doped & undoped composite films were irradiated by two 6W UVL-56 UV lamps. The primary wavelength of the lamps was 365 nm and the light intensity measured with ABM Model 150 digital intensity meter was 1.4 mW/cm² at 3 cm away from the lamps. For artificial light source a common household energy saver bulb of TORNADO 24 watt was used. Table 3 shows the summary of the photo catalyzed

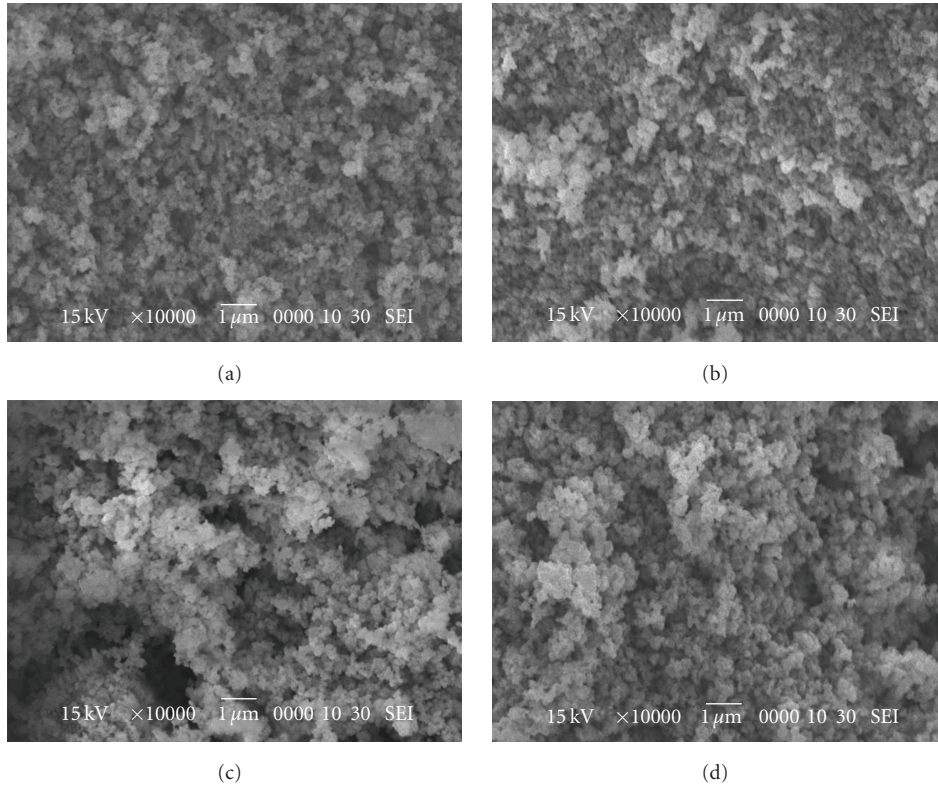


FIGURE 2: SEM images of TiO_2 NPs: (a) undoped TiO_2 , (b) Fe doped TiO_2 , (c) Ag doped TiO_2 , and (d) Fe/Ag mix doped TiO_2 .

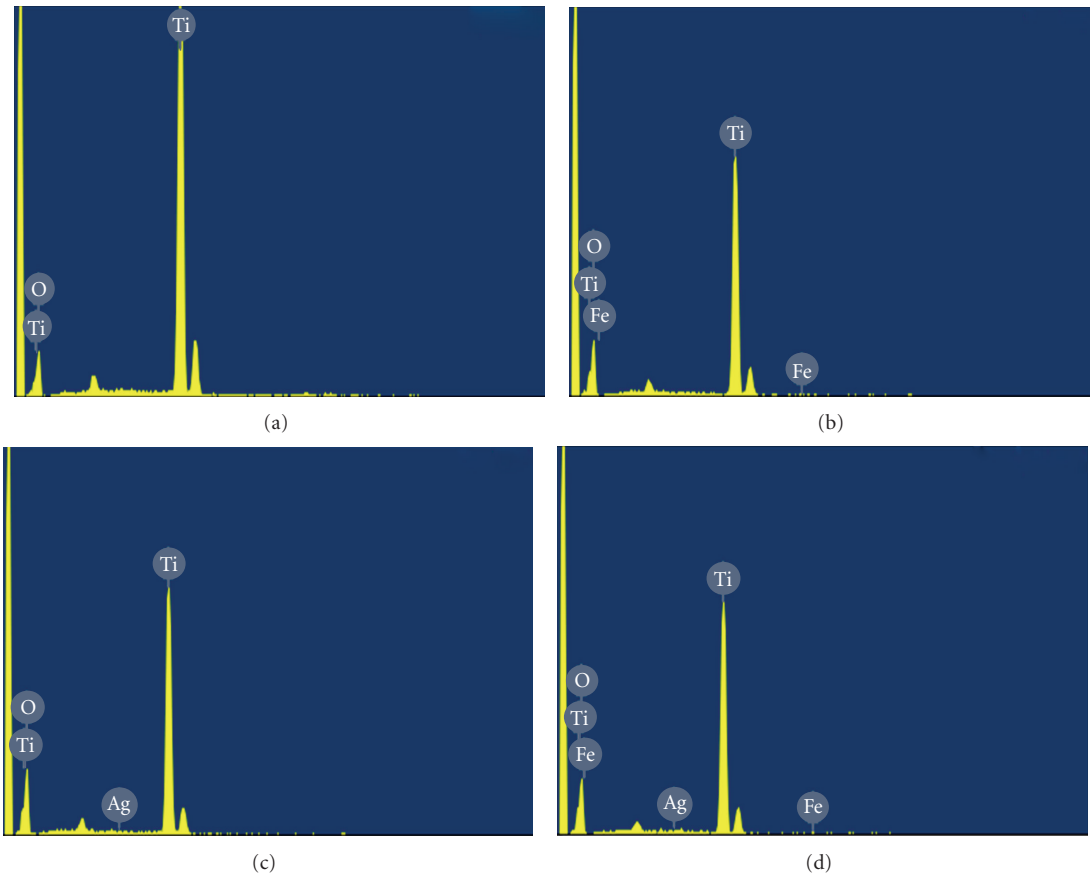


FIGURE 3: EDS spectra of TiO_2 NPs: (a) undoped TiO_2 , (b) Fe doped TiO_2 , (c) Ag doped TiO_2 , and (d) Fe/Ag mix doped TiO_2 .

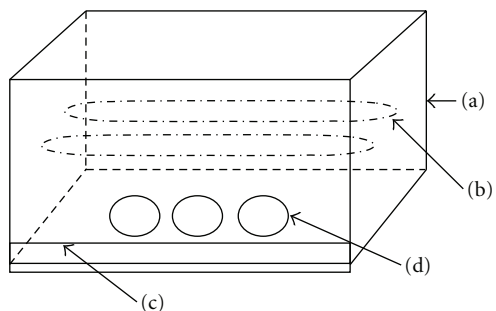


FIGURE 4: Schematic diagram of photocatalytic reactor: (a) lamp housing box, (b) two ultraviolet lamps, (c) air and water inlet, and (d) sample dishes.

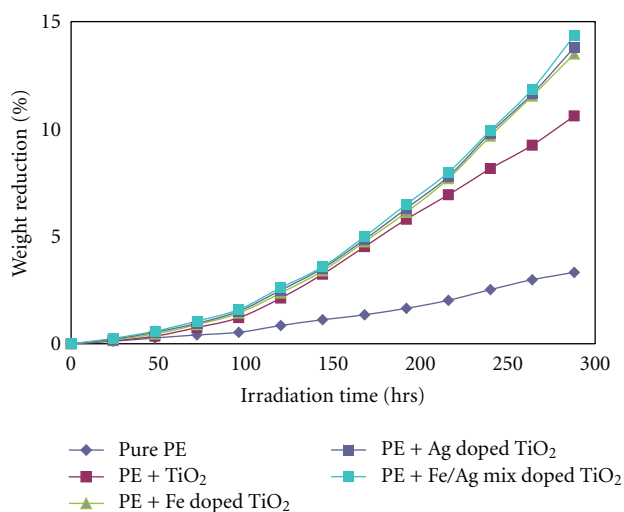


FIGURE 5: Effect of UV irradiation on the photocatalytic degradation of PE films.

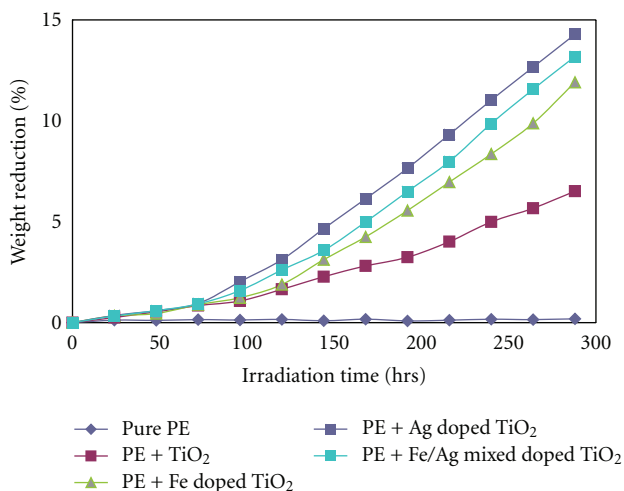


FIGURE 6: Effect of artificial light on the photocatalytic degradation of PE films.

weight loss of pure PE film and PE-TiO₂ composite films with Fe, Ag, and Fe/Ag mix doping under UV irradiation, artificial light and darkness. Figure 5 shows the details of percent weight reduction under UV light and Figure 6 shows the details of percent weight reduction under artificial light. Negligible change was detected in all PE films with or without TiO₂ under darkness.

4.2.2. Polythene Film Thickness. Almost twofold increase in the thickness of polythene films was observed after UV irradiation for 300 hours from 22–28 μm range to 58–61 μm range as shown in Figure 7. This increase in thickness after degradation may possibly be due to the released species like CO₂ causing swelling, affecting the overall thickness of the PE films.

4.2.3. Surface Morphology of Polythene Films. Scanning electron microscope analysis was carried out to observe the surface changes of the films following photo degradation. Figures 8(a) and 8(b) show that the surface of the PE film was smooth before UV irradiation but after UV exposure, due to photo degradation, cavities appeared randomly on the surface of the film. Figures 8(c), 8(d), 8(e), and 8(f) show the texture of PE films with undoped TiO₂, Fe doped TiO₂, Ag doped TiO₂ and Fe/Ag mix doped TiO₂ under UV irradiation, respectively. After irradiation, there were some cavities in the PE film which had also been observed by other workers [14]. The formation of these cavities might be due to the escape of volatile products from PE matrix. More cavities were found on the surface of PE-TiO₂ composite film. Figures 8(c), 8(d), 8(e), and 8(f) show that the degradation is greater than that of PE-TiO₂ composite film. These results were in accordance with the weight loss data shown in Figures 7 and 8. SEM images suggested that the degradation of PE matrix started from PE-TiO₂ interface and led to the formation of cavities around TiO₂ particles. It implied that the active oxygen species generated on TiO₂ surface diffused and degraded the polymer matrix. This is further strengthened by the thickness analysis of the PE films.

4.2.4. Spectroscopic Analysis. Figure 9 shows the FTIR spectra of pure PE films before and after irradiation and PE-TiO₂ (doped and undoped) composite films after UV irradiation. Spectrum of the PE film before irradiation show the characteristic absorption peaks of long alkyl chain in the region of 2919 cm^{-1} , 2857 cm^{-1} , 1475 cm^{-1} , and 715 cm^{-1} . Figures 9(b), 9(c), 9(d), 9(e), and 9(f) show the FTIR spectra of the PE, PE-TiO₂, PE-Fe doped TiO₂, PE-Ag doped TiO₂, and PE-Fe/Ag mix doped TiO₂ after irradiation, respectively. There were new absorption peaks for composite films in the region of 1716 cm^{-1} , 1629 cm^{-1} , and 1175 cm^{-1} , which could be assigned to C=O, C=C and C–O stretching vibrations, respectively [10]. The Peak at 3507 cm^{-1} can be assigned to –OH stretching that may be formed by the hydrolysis reaction.

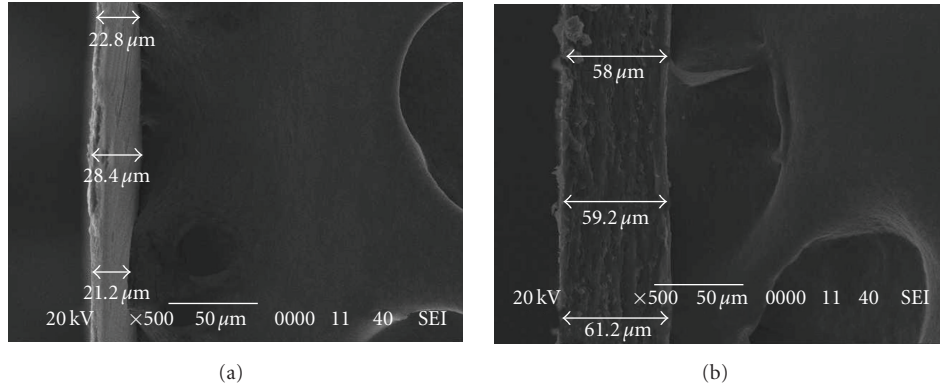


FIGURE 7: Thickness of PE films: (a) before and (b) after irradiation.

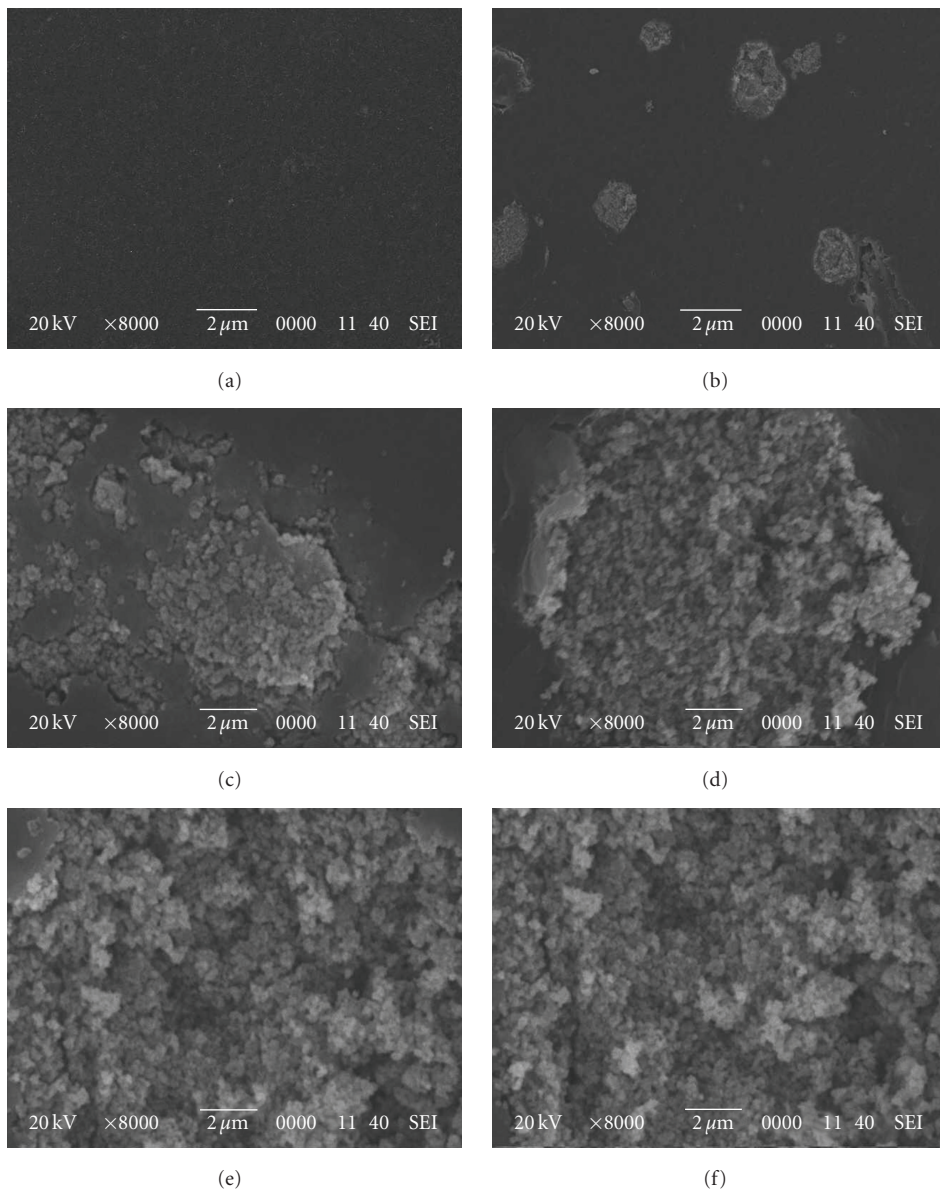


FIGURE 8: SEM images of PE films before and after irradiation: (a) PE film before irradiation, (b) PE film after irradiation, (c) PE-TiO₂ film after irradiation, (d) PE-Fe doped TiO₂ film after irradiation, (e) PE-Ag doped TiO₂ film after irradiation, and (f) PE-Fe/Ag mix doped TiO₂ film after irradiation.

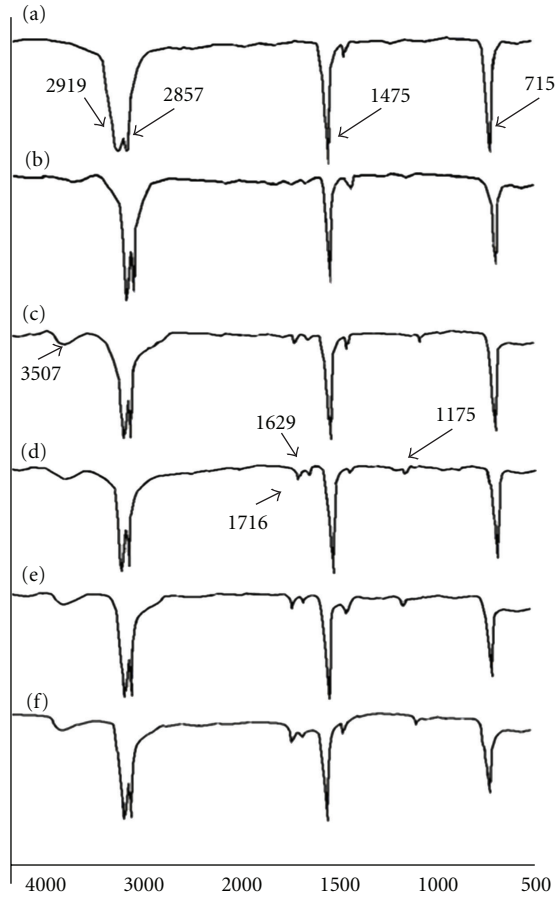
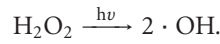
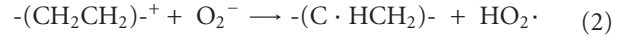
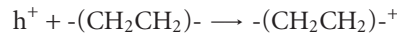
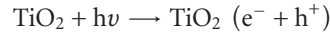


FIGURE 9: FTIR spectra of PE films before and after irradiation: (a) PE film before irradiation, (b) PE film after irradiation, (c) PE-TiO₂ film after irradiation, (d) PE-Fe doped TiO₂ film after irradiation, (e) PE-Ag doped TiO₂ film after irradiation, and (f) PE-Fe/Ag mix doped TiO₂ film after irradiation.

4.2.5. Degradation Mechanism of Polythene Films. Photo degradation of pure PE has been extensively studied [17]. The reaction of pure PE film under UV irradiation occurs via direct absorption of photons by the PE macromolecule to create excited states and then undergo chain scission, branching, cross-linking and oxidation reactions [18]. For composite films, photocatalytic degradation is the main reaction, which is quite different from the photolytic degradation of pure PE film. For PE-TiO₂, the photo degradation of PE mainly happens on the film surface where electrons or holes combine with adsorbed oxygen molecules or hydroxyl ion to produce O₂⁻ or ·OH, two very important reactive oxygen species for the degradation of PE. In the photocatalytic degradation of PE-TiO₂/Fe/Ag, not only O₂⁻ and ·OH but also the holes that are generated in the ground state of Fe/Ag play an important role. Efficient holes production occurs in the ground state of Fe/Ag under irradiation. Although holes in the ground state of Fe/Ag have lower oxidative ability than those in the valence band of TiO₂, it is energetically favorable for these to participate in the oxidation of PE polymer. Further dopants like Fe and Ag can act as both h⁺/e⁻ traps

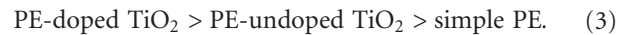
to reduce the recombination rate of h⁺/e⁻ pairs and enhance the photocatalytic activity [19]



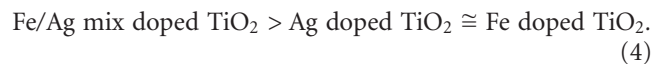
Embedded TiO₂ NPs can generate enough ·OH to photo degrade inner PE. The active oxygen species described above, initiate the degradation reaction by attacking neighboring polymer chains [7]. The degradation process spatially extends into the polymer matrix through the diffusion of the reactive oxygen species. Once the carbon-centered radicals are introduced in the polymer chain, their successive reactions lead to the chain cleavage with the oxygen incorporation and species containing carbonyl & carboxyl groups are produced. These intermediates can be further photo catalytically oxidized to CO₂ and H₂O by the aid of reactive oxygen species [20].

5. Conclusions

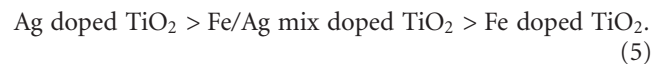
Doping of TiO₂ NPs by Liquid Impregnation method alters its characteristics such as particle size and surface morphology. The effect of mix doping is midway between that of the doping effect by a single metal alone. This indicates that metal ratios can be adjusted to get a desired impact for a particular requirement. This idea was implied and verified in the photo degradation of PE under UV and artificial light irradiation. Photo degradation of PE-TiO₂ films occurred at faster rate and was more complete than the simple photo degradation of pure PE films under UV and artificial light irradiation. Among the PE-TiO₂ films, the degradation of doped TiO₂ composite film was greater than the undoped TiO₂ composite film both under UV and artificial light irradiation. Overall degradation trend can be represented as



Catalytic trend among the doped TiO₂ NPs under UV irradiation can be represented as



Catalytic trend among the doped TiO₂ NPs under artificial light can be represented as



It is our observation that development of this kind of composite polymer can lead to an environmental friendly polythene product.

References

- [1] C.-C. Pan and J. C. S. Wu, "Visible-light response Cr-doped $\text{TiO}_{2-x}\text{N}_x$ photocatalysts," *Materials Chemistry and Physics*, vol. 100, no. 1, pp. 102–107, 2006.
- [2] D. Nabi, I. Aslam, and I. A. Qazi, "Evaluation of the adsorption potential of titanium dioxide nanoparticles for arsenic removal," *Journal of Environmental Sciences*, vol. 21, no. 3, pp. 402–408, 2009.
- [3] C. He, Y. Yu, X. Hu, and A. Larbot, "Influence of silver doping on the photocatalytic activity of titania films," *Applied Surface Science*, vol. 200, no. 1–4, pp. 239–247, 2002.
- [4] M. S. Hegde, K. Nagaveni, and S. Roy, "Synthesis, structure and photocatalytic activity of nano TiO_2 and nano $\text{Ti}_{1-x}\text{M}_x\text{O}_{2-\delta}$ ($\text{M} = \text{Cu}, \text{Fe}, \text{Pt}, \text{Pd}, \text{V}, \text{W}, \text{Ce}, \text{Zr}$)," *Journal of Physics*, vol. 65, no. 4, pp. 641–645, 2005.
- [5] W. Ren, Z. Ai, F. Jia, L. Zhang, X. Fan, and Z. Zou, "Low temperature preparation and visible light photocatalytic activity of mesoporous carbon-doped crystalline TiO_2 ," *Applied Catalysis B: Environmental*, vol. 69, no. 3–4, pp. 138–144, 2007.
- [6] C. Yan, X. Mei, W. He, and S. Zheng, "Present situation of residue pollution of mulching plastic film and controlling measures," *Transactions of the Chinese Society of Agricultural Engineering*, vol. 22, no. 11, pp. 269–272, 2006.
- [7] P. Mormile, L. Petti, M. Rippa, B. Immirzi, M. Malinconico, and G. Santagata, "Monitoring of the degradation dynamics of agricultural films by IR thermography," *Polymer Degradation and Stability*, vol. 92, no. 5, pp. 777–784, 2007.
- [8] A. Sharma and A. Sharma, "Degradation assessment of low density polythene (LDP) and polythene (PP) by an indigenous isolate of *Pseudomonas stutzeri*," *Journal of Scientific and Industrial Research*, vol. 63, no. 3, pp. 293–296, 2004.
- [9] S.-Y. Lee, J.-H. Yoon, J.-R. Kim, and D.-W. Park, "Degradation of polystyrene using clinoptilolite catalysts," *Journal of Analytical and Applied Pyrolysis*, vol. 64, no. 1, pp. 71–83, 2002.
- [10] S. H. Kim, S.-Y. Kwak, and T. Suzuki, "Photocatalytic degradation of flexible PVC/ TiO_2 nanohybrid as an eco-friendly alternative to the current waste landfill and dioxin-emitting incineration of post-use PVC," *Polymer*, vol. 47, no. 9, pp. 3005–3016, 2006.
- [11] S. Chakrabarti, B. Chaudhuri, S. Bhattacharjee, P. Das, and B. K. Dutta, "Degradation mechanism and kinetic model for photocatalytic oxidation of PVC-ZnO composite film in presence of a sensitizing dye and UV radiation," *Journal of Hazardous Materials*, vol. 154, no. 1–3, pp. 230–236, 2008.
- [12] J. Shang, M. Chai, and Y. Zhu, "Solid-phase photocatalytic degradation of polystyrene plastic with TiO_2 as photocatalyst," *Journal of Solid State Chemistry*, vol. 174, no. 1, pp. 104–110, 2003.
- [13] X. U. Zhao, Z. Li, Y. Chen, L. Shi, and Y. Zhu, "Solid-phase photocatalytic degradation of polyethylene plastic under UV and solar light irradiation," *Journal of Molecular Catalysis A*, vol. 268, no. 1–2, pp. 101–106, 2007.
- [14] G. L. Liu, D. W. Zhu, S. J. Liao, L. Y. Ren, J. Z. Cui, and W. B. Zhou, "Solid-phase photocatalytic degradation of polyethylene-goethite composite film under UV-light irradiation," *Journal of Hazardous Materials*, vol. 172, no. 2–3, pp. 1424–1429, 2009.
- [15] M. A. Behnajady, N. Modirshahla, and M. Shokri, "Enhancement of photocatalytic activity of TiO_2 nanoparticles by silver doping: photo deposition versus liquid impregnation methods," *Global NEST Journal*, vol. 10, pp. 1–7, 2008.
- [16] M. H. Habibi, M. N. Esfahani, and T. A. Egerton, "Photochemical characterization and photocatalytic properties of a nanostructure composite TiO_2 film," *International Journal of Photoenergy*, vol. 2007, Article ID 13653, 8 pages, 2007.
- [17] F. Fallania, G. Ruggiera, and S. Broncoci, "Modification of surface and mechanical properties of polyethylene by photo-initiated reactions," *Polymer Degradation and Stability*, vol. 82, pp. 257–261, 2003.
- [18] M. Scoconi, S. Cimmino, and M. Kaci, "Photo-stabilisation mechanism under natural weathering and accelerated photo-oxidative conditions of LDPE films for agricultural applications," *Polymer*, vol. 41, no. 22, pp. 7969–7980, 2000.
- [19] W.-C. Hung, Y.-C. Chen, H. Chu, and T.-K. Tseng, "Synthesis and characterization of TiO_2 and Fe/ TiO_2 nanoparticles and their performance for photocatalytic degradation of 1,2-dichloroethane," *Applied Surface Science*, vol. 255, no. 5, pp. 2205–2213, 2008.
- [20] X. Zhao, Z. Li, Y. Chen, L. Shi, and Y. Zhu, "Enhancement of photocatalytic degradation of polyethylene plastic with CuPc modified TiO_2 photocatalyst under solar light irradiation," *Applied Surface Science*, vol. 254, no. 6, pp. 1825–1829, 2008.



Hindawi

Submit your manuscripts at
<http://www.hindawi.com>

